

## Microstructure of calcined Mg-rich clay minerals of Egyptian serpentinites

HASSAN MERVAT

Central Metallurgical R &amp; D Institute, P.O. Box 87, Helwan, Cairo, Egypt

*Submitted, July 2007 - Accepted, February 2008*

**ABSTRACT.** — The thermal behaviour of Mg-rich clay minerals in two serpentinites was studied by means of DSC-TG, XRD, IR and SEM. Experiments are carried out heating at temperatures in the 600-1200 °C range for 2-4 hours. Analyses revealed that antigorite, talc and clinocllore are the main Mg-rich clay minerals. Dolomite and magnesite are accessory minerals. Chromite, magnetite and hematite are in small amounts. DSC-TG results of the antigorite-rich sample reveal that most of the loss of free water and water absorbed at surface (approx. 13%) occurs at approximately 750 °C. The decomposition into the high-temperature products forsterite + enstatite proceeds via an intermediate assemblage of forsterite and a talc-like phase, observed within a temperature interval of  $100 \pm 20$  °C. The breakdown of antigorite and the talc-like phase is kinetically controlled by surface growth processes at the edges of grains. The decomposition of the talc-clinocllore-antigorite assemblage took place at higher temperature and produced enstatite and spinel. It is suggested that their formation depends on how clinocllore dehydrates and on the talc trioctahedral arrangement, which provides rapid transformation into enstatite. The increase of the reaction rate with temperature is confirmed by XRD and IR data as well as by SEM. Results of this work, indicate that highly crystalline

forsterite and enstatite form by dehydroxylation of Mg-rich minerals.

**RIASSUNTO.** — Il comportamento termico di minerali argillosi ricchi di Mg presenti in due serpentiniti è stato analizzato tramite l'uso di apparecchiature quali DSC-TG, XRD, IR e SEM. Gli esperimenti sono stati condotti riscaldando il materiale a temperature comprese tra 600 e 1200 °C per intervalli di tempo variabili da 2 a 4 ore.

Dalle analisi è emerso che i principali minerali ricchi di Mg sono antigorite, talco e clinocllore. Dolomite e magnesite figurano come accessori mentre cromite, magnetite ed ematite sono presenti in quantità modeste.

I risultati delle analisi DSC-TG relative ai campioni ricchi di antigorite hanno evidenziato che la maggior parte delle perdite dell'acqua libera e di quella assorbita dalla superficie (intorno al 13%) avviene a circa 750 °C; la trasformazione nei materiali di alta temperatura forsterite + enstatite si realizza tramite prodotti intermedi quali forsterite ed una fase simile al talco in un intervallo termico di  $100 \pm 20$  °C. I collassi dell'antigorite e della fase simile al talco sono controllati, sotto il profilo cinetico, da processi di crescita superficiale lungo gli spigoli dei granuli. La trasformazione dell'insieme costituito da talco-clinocllore-antigorite si verifica a temperature più elevate e produce enstatite e spinello; sembra che la loro

formazione dipenda dalle modalità di disidratazione del clinocloro e dalla ristrutturazione triottaedrica del talco che facilita la rapida trasformazione in enstatite. L'aumento della velocità di trasformazione con la temperatura è stata confermata dalle indagini XRD, IR e al SEM.

I risultati di questo lavoro indicano che forsterite ed enstatite con alto grado di cristallinità derivano dalla deossidrilizzazione di minerali ricchi di Mg.

**KEY WORDS:** *Eastern Desert, Egypt, serpentinites, antigorite, talc, clinocllore, dehydration, forsterite, enstatite.*

### INTRODUCTION

Clay minerals are widely used in a range of applications, such as ceramics and refractory materials, foundry binding sands, paper production, as catalysts or additives for polymeric materials, barriers in toxic and nuclear waste deposits etc. The overall firing properties of the clay depend on the firing properties of the individual clay minerals species which can be plotted on a time-temperature-transformation (TTT) diagrams (Dunham *et al.*, 1992; Barlow *et al.*, 2000). The dehydroxilation peak temperature of trioctahedral minerals (serpentine group) is higher than that of dioctahedral minerals (kaolinite). In contrast, the peak temperature of the exothermic recrystallization is lower in trioctahedral minerals because of the lower stability of the dehydroxilate (Taylor, 1962).

The purpose of this study was to determine the firing behavior of serpentine rocks (and their mineral association) from ophiolitic successions of the Eastern Desert of Egypt in order to provide an experimental basis for their exploitation and utilization. Chemical analysis, X-ray diffraction (XRD), infrared spectroscopy (IR), differential scanning calorimetry (DSC), thermogravimetry (TG) and Scanning electron microscopy (SEM) were applied to study serpentine minerals and their heated products.

### MATERIALS AND METHODS

The two investigated samples (Wa from Wadi At-Attalh and Br from El Barramiya) are antigorite

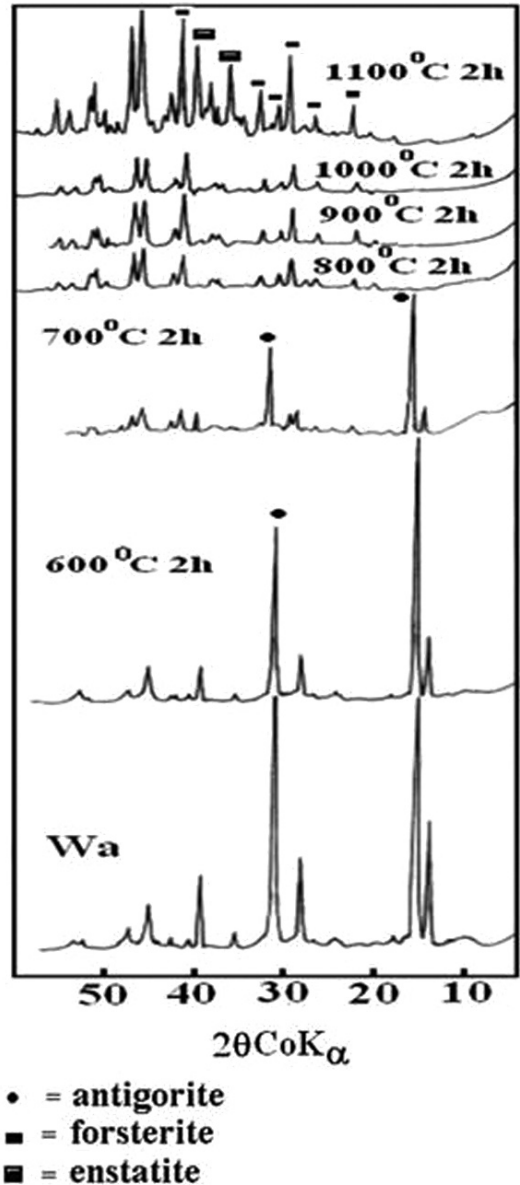


Fig. 1 – XRD patterns of serpentine (Wa) heated at temperatures of 600–1100 °C for 2 h.

and talc-clinocllore-antigorite serpentinites from the Eastern Desert of Egypt. Mineralogy of the serpentine minerals and their heated products

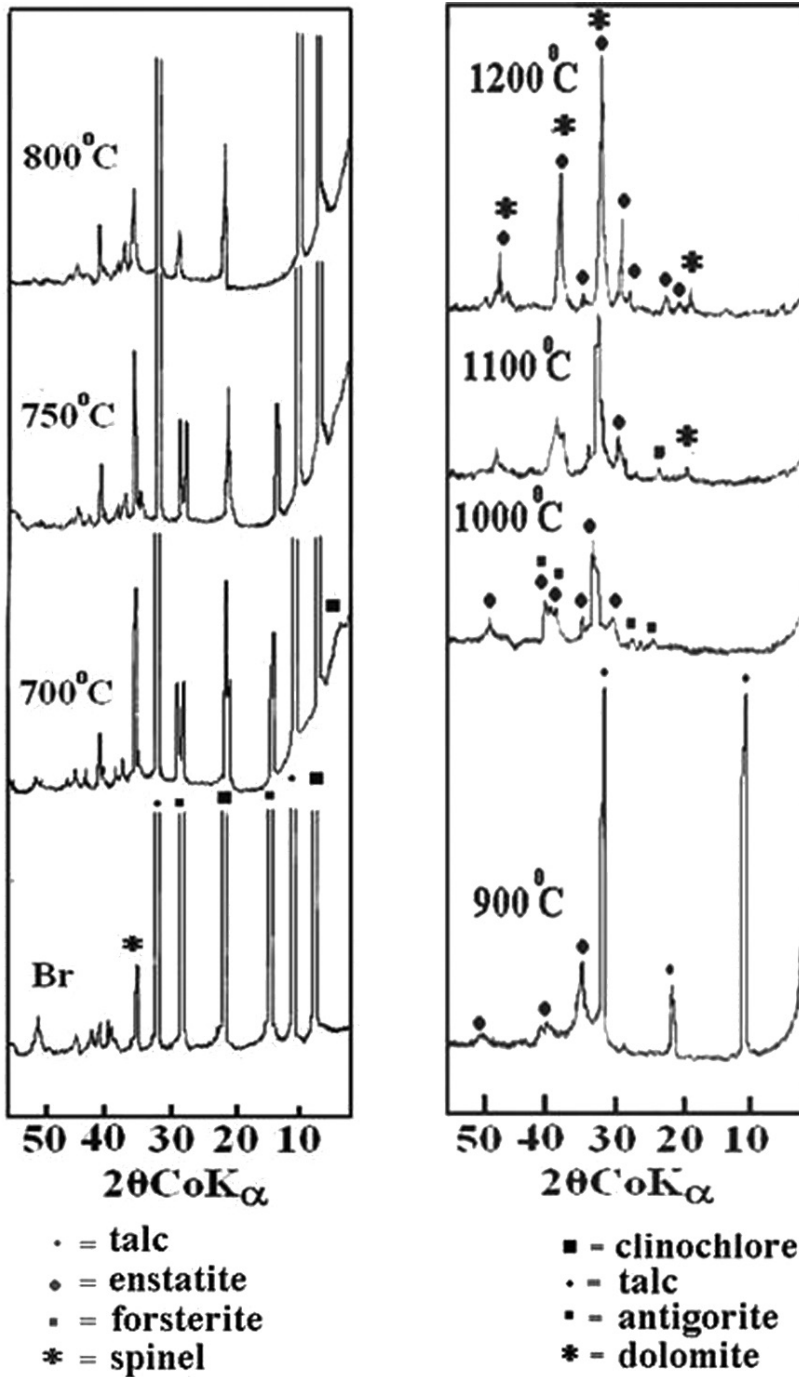


Fig. 2 – XRD patterns of serpentinite (Br) heated at temperatures of 700–1200 °C for 2 h.

TABLE 1  
Powder x-ray diffraction data of studied samples

Wa	Br	
dÅ	dÅ	
14.25	14.25	Cl
—	9.33	Ta
7.3	7.34	An
6.59	—	An
—	4.73	Cl
4.64	4.65	An
—	4.54	Ta
4.25	—	Qz
3.64	3.62	An
350	3.52	Cl
3.37	—	Qz
—	3.11	Ta
3.04	—	Ca
2.97	—	Mag,Ch
2.89	2.88	Do
—	2.83	Ha
2.74	—	Mags
—	2.62	Ta
—	2.59	Ta
2.53	—	An,Mag,Ch
2.47	2.47	An,Ta
2.43	—	Do
—	2.33	Cl
2.29	—	An
—	2.21	Ta
2.19	—	Do
2.18	—	An
2.15	—	Ch,Mags
2.09	2.1	Ch,Mag,Ta
2.02	2.02	Do,Ta
—	1.86	Ta
1.83	—	Do
1.81	—	An
1.8	—	An
1.78	—	An,Do
1.71	1.72	Mags,Ta
—	1.68	Ta
—	1.67	Ta
1.64	—	An
1.57	1.55	An,Ta
1.54	1.52	An,Ta
1.48	—	Ch,Mag

was determined by means of a PW 1170 Phillips diffractometer with CoK $\alpha$  radiation on randomly oriented specimens. The samples were scanned from 4 to 60 2 $\theta$ . The IR spectra were obtained using a Bruker FTIR spectrometer. On each sample 128 scans were recorded in the 4000–400 cm<sup>-1</sup> spectral range in the transmittance mode, with resolution of 4 cm<sup>-1</sup>. The KBr pressed disk technique was used.

DSC and TG measurements were carried out on a Setaram simultaneous thermal analysis apparatus (Labsys<sup>TM</sup> TG-DSC 1600 °C). Approximately 20 mg of sample were placed in a platinum pan and heated over a temperature range 30–1000 °C, at 10 °C/min, under ultrahigh purity argon atmosphere. The morphology of serpentine minerals and their heated product was studied by means of a Philips S-2400s SEM at the Geological Survey of Egypt.

## RESULTS AND DISCUSSION

### Sample Composition

The only serpentine mineral in sample Wa is antigorite. Its strongest peaks on the XRD pattern (Fig. 1) are at 7.3, 3.6 and 2.5 Å. The distinguishing feature to recognize antigorite from other serpentine minerals is the 1.56–1.57 Å peak, which is only found in antigorite minerals (Whittaker and Zussman 1956). Traces of clinochlore, calcite and quartz were recorded in sample Wa. Antigorite, talc and clinochlore (Fig. 2) are the main components of sample Br. Both samples contain dolomite and magnesite and small amounts of chromite, magnetite and hematite (Table 1). In Table 2 are the results of the chemical analysis of the two samples.

### XRD DETERMINATION OF PHASE TRANSITIONS

In Fig. 1 are the XRD patterns obtained from heated products of sample Wa. The (001) and (002) reflections of antigorite are still observed after treatment for 2h at 700 °C though with decreasing

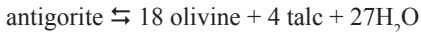
An = Antigorite; Ca = Calcite; Ch = Chromite; Cl = Clinochlore; Do = Dolomite; Ha = Halite; Mags = Magnesite; Mag = Magnetite; Qz = Quartz; Ta = Talc

TABLE 2  
Chemical composition of serpentinite samples

	SiO <sub>2</sub>	TiO <sub>2</sub>	Al <sub>2</sub> O <sub>3</sub>	Fe <sub>2</sub> O <sub>3</sub>	MgO	CaO	NaO <sub>2</sub>	K <sub>2</sub> O	P <sub>2</sub> O <sub>5</sub>	SO <sub>3</sub>	L.O.I
Wa	40.13	--	0.97	4.51	38.1	2.62	0.05	0.058	0.032	0.05	13.16
Br	41.89	0.85	8.96	9.35	28.2	0.083	0.05	0.004	0.02	--	10.52

peak intensities (2 $\theta$  14.7, 31.3). Above 800 °C, the progressive breaking down of the layered structure occurs.

At 700 °C, new diffraction peaks appear while a broad feature at 6-10° 2 $\theta$  indicates some sort of a layer formation. These reflections are attributed to a forsterite and a phyllosilicate structure (talclike phase) respectively. According to Ulmer and Trommsdorff (1995) the main reaction is the initial breakdown of serpentine under low-pressure conditions into olivine and talc:



From 800 to 1000 °C a sudden increase in the intensity and sharpness of forsterite reflections (2 $\theta$  28.9, 40.9) occurred and increased in samples heated for 2h at 1100 °C. Similar results are reported in literature (Cheng *et al.*, 2002; Seipold and Schilling, 2003 and Phillippe *et al.*, 2005). As shown in Fig. 3, increasing the heating time from 2 to 4 h, the intensities of forsterite and enstatite peaks increased sharply at 1000 °C.

XRD patterns of the heated products from sample Br are in Figure 2. Fired assemblages between 700-800 °C reveal a reduction of the antigorite reflections intensities, which disappear at 800 °C. However, meta-clinocllore has a distinctive set of X-ray diffraction peaks which corresponds to the original clinocllore peak positions. A peak in the original position of the clinocllore (001) (~14Å d-spacing) is greatest in relative intensity after heating at 800 °C for two hours. A new peak develops at about 3.65° 2 $\theta$  (28.5Å d spacing) as also observed by Brindley and Chang (1974). The ~28 Å d-spacing corresponds to the distance between two unit cell sheets. The 14 Å peak is related to the original clinocllore structure, with variation in its intensity as a result of the ordering to produce a rigid layered structure (Brindley and Chang, 1974; Cho and Fawcett, 1986; Villieras *et al.*, 1993). Brindley and Ali (1950) argued that the 14 Å peak develops due to the dehydration of the

'brucite' layer within the clinocllore structure. The dehydration is believed to force the MgO in the 'brucite' layers into a rigid and planar alignment that forms an extremely well-ordered 14Å spacing.

With increasing temperature from 800 to 900 °C, a sudden decrease in the intensity of talc reflections was recognized and poorly crystallized enstatite begins to form. At high temperatures (1000-1100 °C) enstatite reflections appear and get sharper with increasing temperatures. Beside enstatite, traces of forsterite and spinel might be present. At 1200 °C, the forsterite disappears and well crystallized enstatite and spinels were recognized.

#### IR ANALYSIS

The IR spectrum of serpentinite Wa (Fig. 4) is typical of the trioctahedral character of the antigorite structure with three well defined spectral regions; 3800-3600 cm<sup>-1</sup>, 1200-800 cm<sup>-1</sup> and below 800 cm<sup>-1</sup>. The two bands at 3675-3684 (strong) and 3654 cm<sup>-1</sup> (weak) according to Mellini *et al.*, (2002), are related to the inner and outer OH stretching and could be attributed to the presence of two crystallographically different OH groups in the antigorite structure.

In the 1100-900 cm<sup>-1</sup> region, there are two bands (1078 and 988 cm<sup>-1</sup>) and a shoulder (957 cm<sup>-1</sup>) in agreement with literature data (Stubican and Roy, 1961). The highest energy band arises from the Si-O<sub>nb</sub>-Si stretching vibration, whereas the band at 988 cm<sup>-1</sup> is due to Si-O<sub>b</sub> stretching vibration. The shoulder at 957 cm<sup>-1</sup> probably implies slightly different structural Si-O-Si bridging configuration in the antigorite. The band at 620 cm<sup>-1</sup> accompanied with a shoulder at 640 cm<sup>-1</sup> arises from the deformation of R<sup>2+</sup>O-H bonds (R<sup>2+</sup> mainly Mg); the first from the inner, whereas the second from the external O-H bonds. The shoulder at 3571 cm<sup>-1</sup>

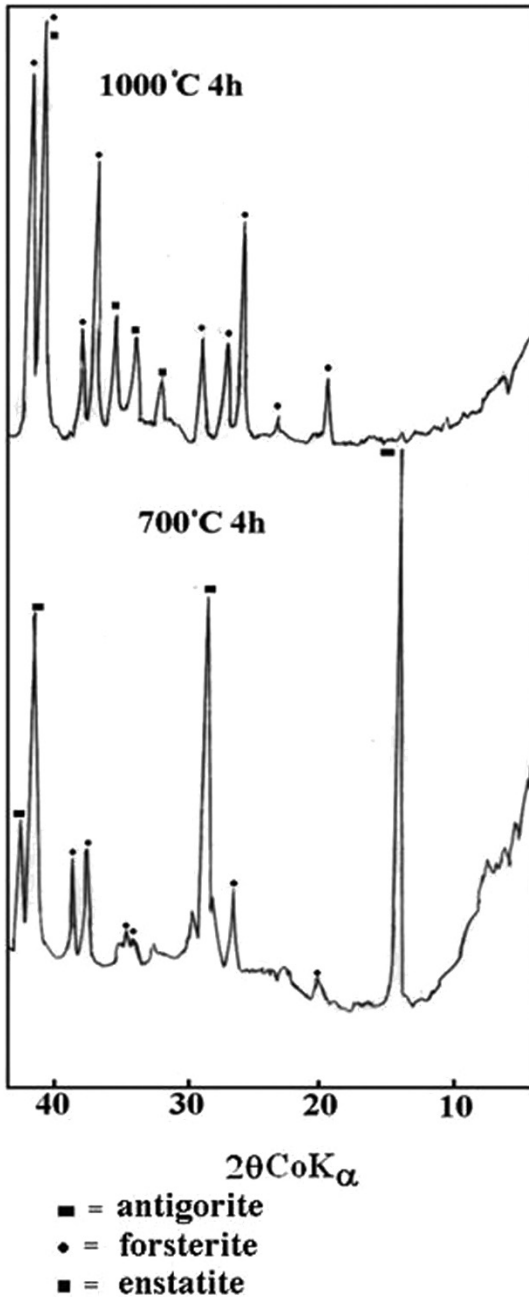


Fig. 3 – XRD patterns of serpentinite (Wa) heated at temperatures of 700–1000 °C for 4 h

may be attributed to traces of clionchlore, whilst at  $1437 \text{ cm}^{-1}$  is the effects of the carbonate minerals.

By heating, the bands of antigorite (Fig. 4) were drastically reduced and disappeared at  $800 \text{ }^\circ\text{C}$  together with a shift of the Si-O-Si related peaks to a lower wave number. The lower wave number is caused by strengthening of Si-O bands in the  $\text{SiO}_4$  tetrahedron at the temperature where forsterite is formed. The bands related to the peaks of forsterite appear in the range of  $883\text{--}1007 \text{ cm}^{-1}$  ( $\text{SiO}_4$  stretching),  $519\text{--}624 \text{ cm}^{-1}$  ( $\text{SiO}_4$  bending) and  $424 \text{ cm}^{-1}$  (octahedral  $\text{MgO}_6$ ). Similar results are also reported in previous studies (Philippe *et al.*, 2005). Heating to  $1200 \text{ }^\circ\text{C}$  induces the appearance of bands related to enstatite  $1074\text{--}729$  and  $685 \text{ cm}^{-1}$  (Fig. 4). As shown in Fig. 5, increasing the heating time from 2 to 4 h, the intensities of forsterite and enstatite peaks increased sharply at  $1000 \text{ }^\circ\text{C}$ .

The infrared spectrum of sample Br shows typical characteristic bands of clinochlore (Fig. 6). The appearance of three bands due to the  $\nu(\text{OH})$  stretching vibrations was connected with the same number of the crystallographically different OH groups present in its structure. The  $3675 \text{ cm}^{-1}$  arises from the vibrations of OH groups not involved in hydrogen bonds (OH groups from 2:1 layer). The remaining more intense two bands (at  $3568$  and  $3424 \text{ cm}^{-1}$ ) were ascribed to hydroxyl groups involved in hydrogen bonds, “(SiAl O...HO and (SiSi)O...OH), respectively (Prieto *et al.*, 1991). The OH-stretching vibration band of antigorite and talc are observed at  $3675 \text{ cm}^{-1}$ . The band at  $988 \text{ cm}^{-1}$  is corresponding to Si-O vibration mode of antigorite. Bands at  $1018$ ,  $466$  and  $669 \text{ cm}^{-1}$  were assigned to  $\nu_1(\text{Si-O-Si})$  mode and OH liberation of talc respectively (Russell *et al.*, 1994). At  $900$  and  $1200 \text{ }^\circ\text{C}$  the clinochlore and antigorite bands disappeared whilst the talc bands still persist up to  $900 \text{ }^\circ\text{C}$  when enstatite peaks started to show at  $648$  and  $480 \text{ cm}^{-1}$ . Above  $1100 \text{ }^\circ\text{C}$ , the bands related to well-crystallized enstatite appear at  $1076$ ,  $1018$ ,  $955$ , and  $893 \text{ cm}^{-1}$  ( $\text{SiO}_4$  stretching),  $648 \text{ cm}^{-1}$  ( $\text{SiO}_4$  bending), and  $480 \text{ cm}^{-1}$  for modes of octahedral MgO. Spinel ( $\text{Mg Al}_2\text{O}_4$ ) characteristic bands appear at  $1018$  and  $685 \text{ cm}^{-1}$  (Fig. 6).

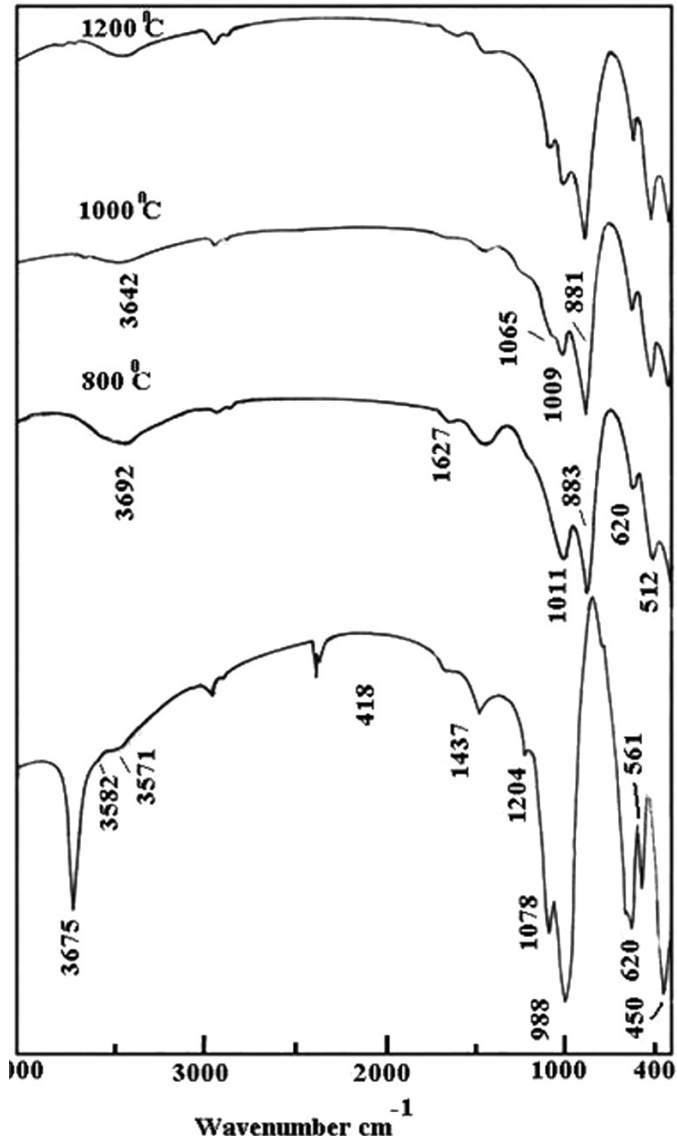


Fig. 4 – IR spectra of serpentinite (Wa) heated at temperatures 800 – 1200 °C for 2h.

#### MICROSTRUCTURE

Sample (Wa) heated at 700 °C induces partial dehydration of primary antigorite to forsterite and a talc-like phase. This reaction generates considerable porosity and micrometer-scale cracking in the surrounding antigorite. Narrow cracks appear to connect separate reaction zones

and may be conduits for fluid flow through the sample (Eric and Stephen, 2003). The breakdown of antigorite and the talc-like phase is kinetically controlled by surface growth processes occurring at the grains edges. In all the experiments conducted above 700 °C, the secondary products appear as an interwoven, fibrous mosaic of individual forsterite and talc grains which are difficult to distinguish

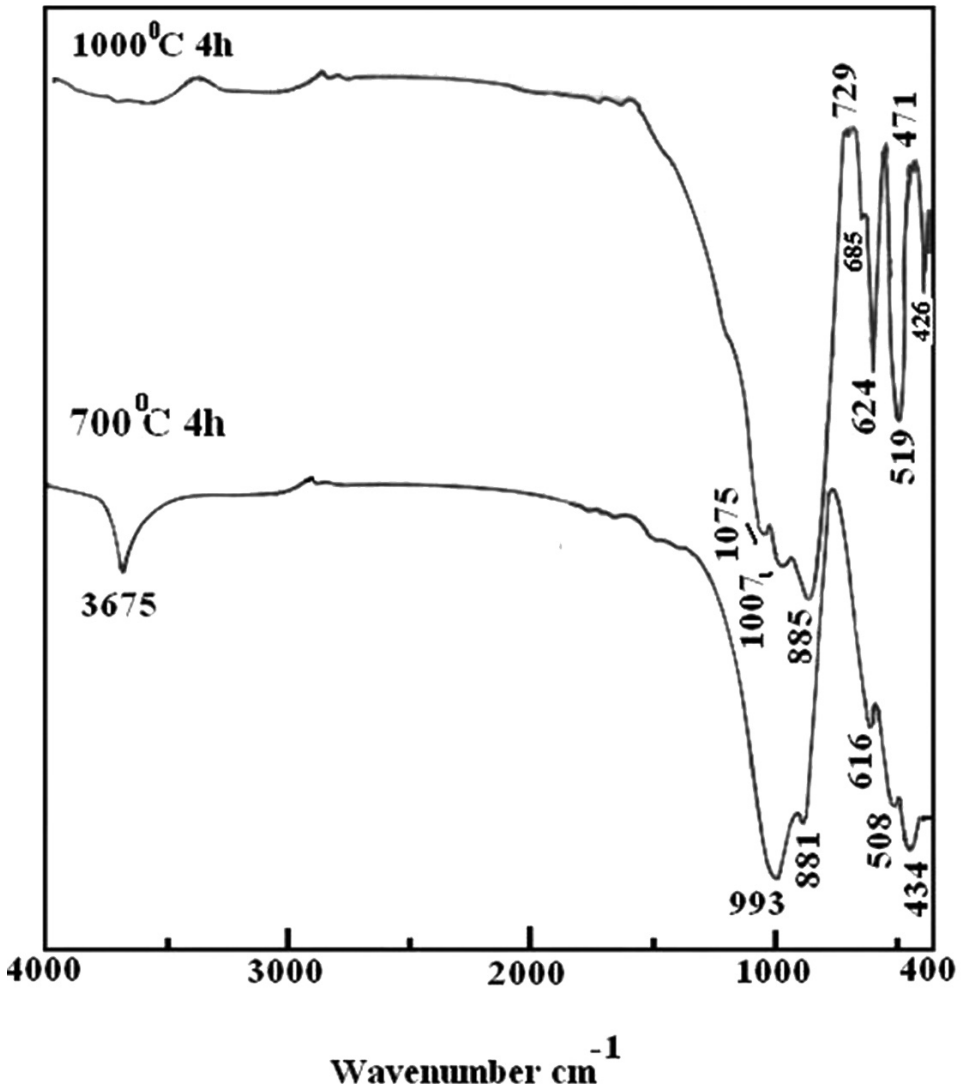


Fig. 5 – IR spectra of serpentinite (Wa) heated at temperatures 700 – 1000 °C for 4h

under the SEM. Large euhedral crystals of enstatite derived from the reaction of free magnesia and silica at 1100 °C are recognized in the fired product.

Phases transformation of the talc, clinochlore and antigorite assemblage of sample Br are showing in Fig. 8. At 900 °C, enstatite crystals with fibrous and lamellar texture are derived from

clinochlore and antigorite. At 1200 °C, clusters of prismatic crystals of ferroenstatite were formed by dehydration of talc. The reaction of alumina from the tetrahedral sites of clinochlore formed spinel ( $MgAl_2O_4$ ) together with enstatite. The new enstatite has a distinctly fibrous fine-grained form.

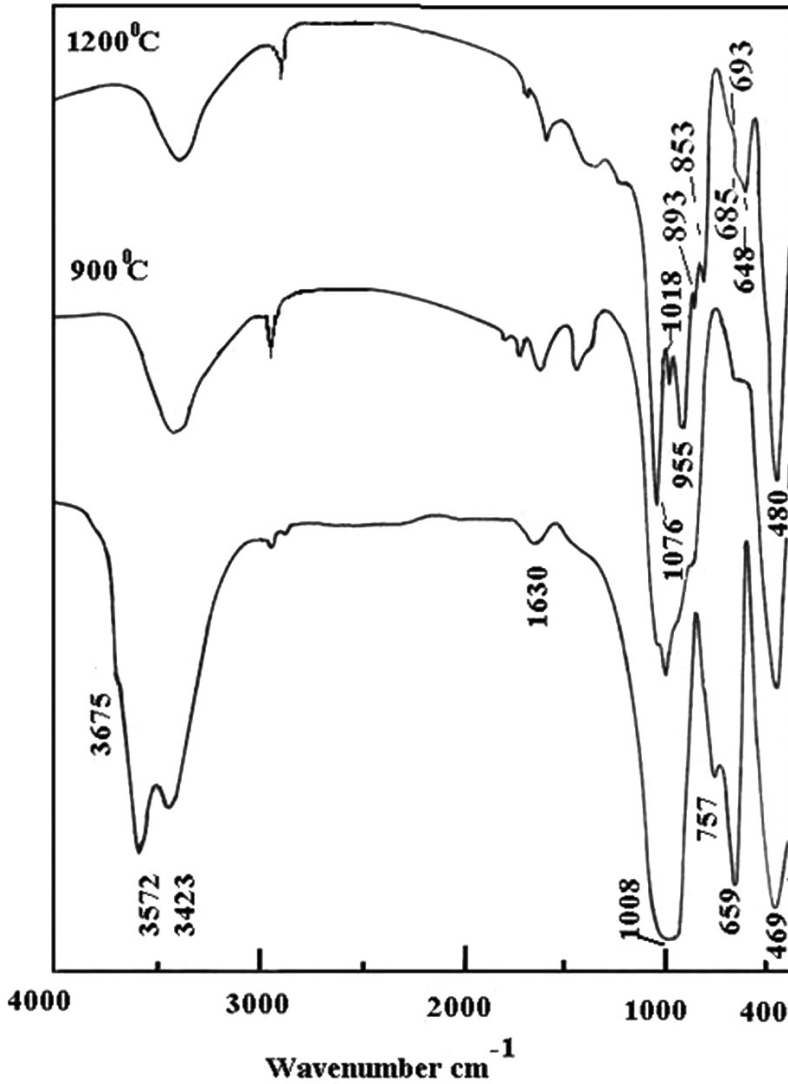


Fig. 6 – IR spectra of serpentinite (Br) heated at temperatures 900 – 1200 °C for 2h.

#### DSC/TGA ANALYSES

Upon heating, antigorite  $\text{Mg}_6\text{Si}_4\text{O}_{10}(\text{OH})_8$  dehydrates to forsterite ( $\text{Mg}_2\text{SiO}_4$ ) and a talc-like phase ( $\text{Mg}_3\text{Si}_4\text{O}_{10}(\text{OH})_2$ ). The dehydration of talc and the reaction with forsterite lead to enstatite ( $\text{MgSiO}_3$ ). On the TG-DSC curves (Fig. 9) two overlapping endothermic reactions occur during the dehydration of antigorite, a strong one at ~

759 °C followed by a shoulder. The weight loss is 13.5%. The dehydration peaks of antigorite are closely followed by an exothermic peak related to the formation of forsterite, as confirmed by XRD.

According to Taylor, 1962, dehydroxilation occurs by an inhomogeneous mechanism. Dolomite gives two separated thermal behaviors; the first reaction is situated at 805 °C and includes the transformation of carbonate bonded with

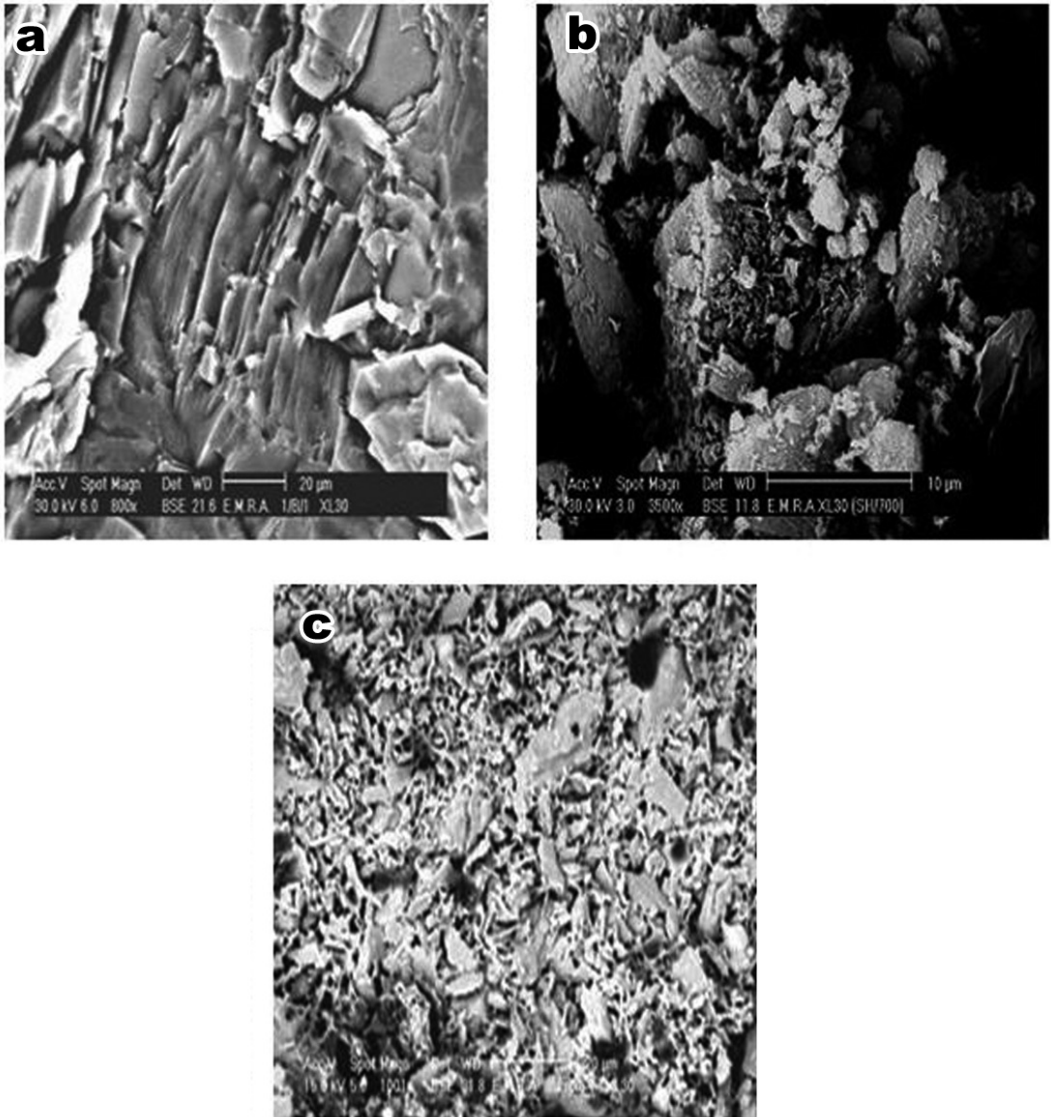


Fig. 7 – SEM micrograph of serpentinite (Wa) heated at temperatures 700 – 1200 °C 2 h.  
a = original; b = 700 °C; C = 1200 °C.

magnesium and the second effect observed at 850 °C attributed to the decomposition of carbonate ions associated with calcium (broad endothermic peak appears between 805-850 °C).

The two steps of the dehydration reactions are clearly resolved in the DSC curve. In the TG

curve, both dehydration reactions overlap and are visible as a change in the dehydration curve (Fig. 9). The dehydration reaction and crystallization of the products are kinetically hindered (Faust and Fahey, 1962). Amorphous material is revealed by XRD, the temperature range between dehydration

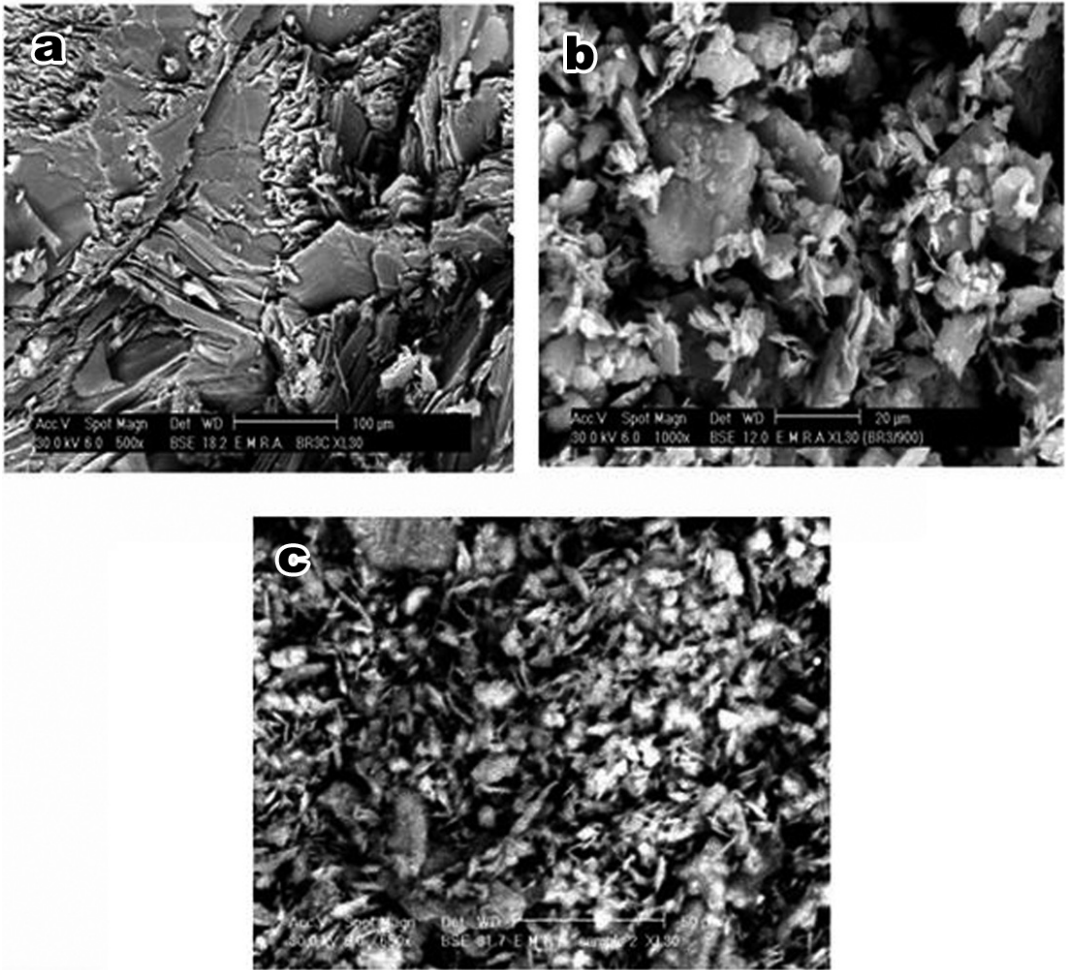


Fig. 8 – SEM micrograph of serpentinite (Br) heated at temperatures 700- 1200 °C for 2h  
a = original; b = 700 °C; C = 1200 °C

and crystallization of forsterite (endothermic peak at low temperature in DSC curve of preheated sample at 800 °C).

DSC-TG curves of sample Br and its heated products are showing in Fig. 10. Clinocllore has two large endothermic dehydroxilation peaks. The first at 619 °C followed by an end-exothermic at 839-857 °C. According to Brindley and Ali (1950) when clinocllore is heated above 800 °C, forsterite forms first followed by spinel and enstatite. Brindley and Chang (1974) observed

two weight loss steps which correspond to the water content of the 'talc' and the 'brucite' layers of the clinocllore structure. They suggested that the 'brucite' layer dehydrates before the water is lost from the 'talc' layer. The development of an X-ray peak at 27Å and a significant increase in the intensity of the (001) clinocllore peak are attributed to the repositioning of the MgO within the octahedral 'brucite' layer.

XRD of fired products of sample Br show an anhydrous assemblage of enstatite, forsterite and

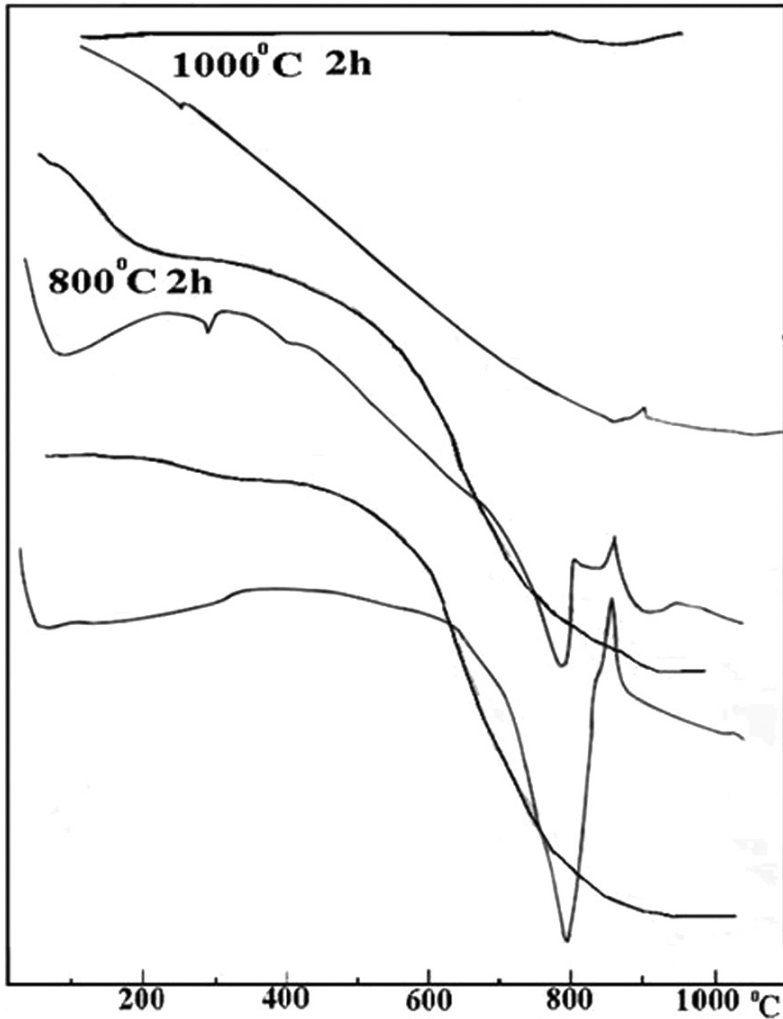


Fig. 9 – DSC/TG curves of serpentinite (Wa) heated at temperatures 800- 1000 °C for 2h.

spinel (Fig. 11) which is identical to the phase assemblage produced in the TTT diagram of Barlow *et al.*, (2000).

The mechanism for the development of this assemblage is thought to be dependent

on the way in which clinochlore dehydrates (Barlow *et al.*, 2000). It is suggested that the initial dehydration of the ‘brucite’ layer of clinochlore during the calcinations does not produce an environment suitable for the nucleation of any

new phases. Instead a long range order develops within the layer structure, as suggested by the development of the  $\sim 28.5\text{\AA}$  reflection. When the ‘talc’ layer loses its water, silica and alumina become available to react with the MgO freed from the ‘brucite’ and from antigorite which is dehydrated at  $\sim 700\text{ }^\circ\text{C}$ . As the reaction proceeds with further disruption of the silica-rich tetrahedral layer, enstatite ( $\text{Mg}_2\text{Si}_2\text{O}_6$ ) begins to form at  $900\text{ }^\circ\text{C}$ . Talc begins to dehydrate at about  $963\text{ }^\circ\text{C}$ . The



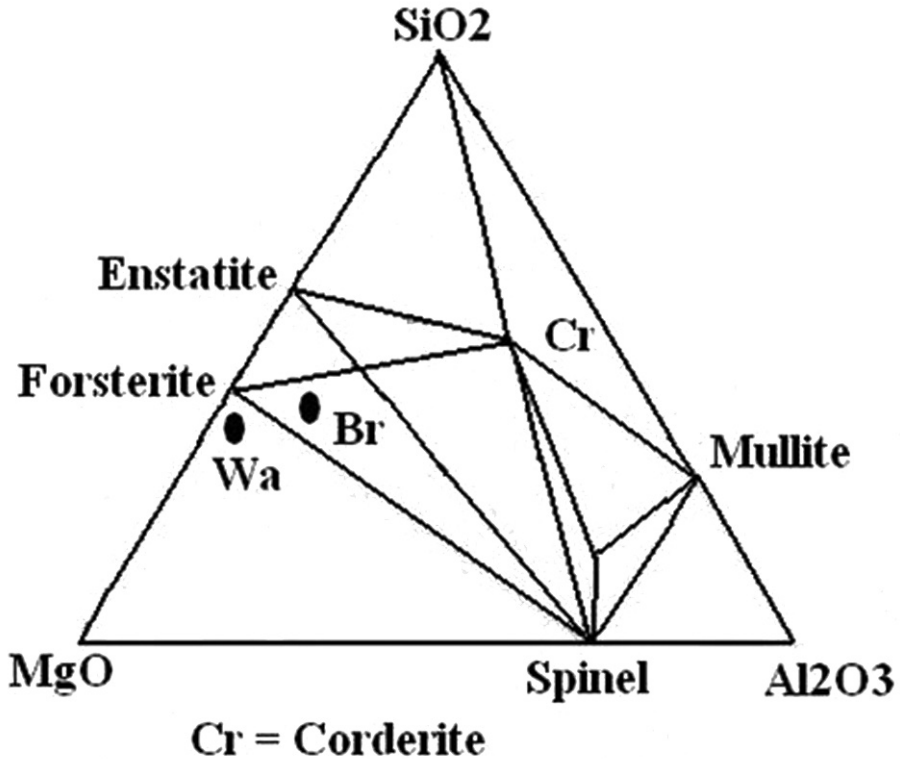


Fig. 11 – Phase relationships for the ternary system MgO - Al<sub>2</sub>O<sub>3</sub> - SiO<sub>2</sub> (Roy and Roy, 1955) at 1200 °C, showing the starting composition for serpentinites and compositions of products fired at 1200 °C for 2h.

forms spinel (MgAl<sub>2</sub>O<sub>4</sub>) which develops jointly with the enstatite, as the XRD evidence suggests.

#### CONCLUSIONS

The analyses carried out on two serpentinites demonstrated that heating Mg-rich minerals highly crystalline forsterite and enstatite may be produced. They crystallize from 800 °C to 1200 °C from the decomposition of antigorite, talc and clinocllore. The breakdown of antigorite of sample Wa occurs as a two-step process during heating; at low temperatures antigorite → forsterite + “talc-like” phase + H<sub>2</sub>O; at higher temperature forsterite + “talc-like” phase → enstatite + H<sub>2</sub>O. The peak intensities of forsterite and enstatite increased with rising temperature implying higher crystallinity.

The decomposition of the talc-clinocllore-antigorite assemblage of sample Br take place at higher temperature and produces enstatite and spinel. It is suggested that the formation depends on the way in which clinocllore dehydrates and on the talc trioctahedral arrangement, which provides rapid transformation into enstatite. No quartz was observed XRD measurements, which would appear for samples with excess in talc only.

#### REFERENCES

- BARLOW S.G., MANNING D.A.C. and HILL P.I (2000) - *The influence of time and temperature on the reactions and transformations of clinocllore as ceramic clay mineral*. Int. Ceram., **2**, 5-10.
- BRINDLEY G.W. and CHANG T.S. (1974) - *Development of long basal spacing in chlorites by thermal*

- treatment. *Am. Mineral.*, **59**, 152-158.
- BRINDLEY G.W. and ALI S.Z. (1950) - *X-ray study of thermal transformations in some magnesium chlorite minerals*. *Acta Crystall.*, **3**, 25-30.
- CHENG T.W., DING Y.C. and CHIU J.P. (2002) - *A study of synthetic forsterite refractory materials using waste serpentine cutting*. *Mineral. Engin.*, **15**, 271-275
- CHO M. and FAWCETT J.J. (1986) - *Morphologies and growth mechanisms of synthetic Mg-chlorite and cordierite*. *Am. Mineral.*, **71**, 78-84
- DUNHAM A.C., MCKNIGHT A.S. and WARREN I. (1992) - *The determination and application of Time-Temperature-Transformation diagrams for brick, tile and pipe clays*. Final report to the Mineral Industry Research Organization of Project RC56: TTT Diagrams for Brick, Tile and Pipe Clays.
- ERIC T. and STEPHEN F.C. (2003) - *Reaction-enhanced permeability during serpentinite dehydration*. *Geology*, 920-924
- EVAN B.W. and GUGGENHEIM S. (ed.), (1988) - *Talc, pyrophyllite and related minerals*: In *Hydrous phyllosilicates (exclusive micas)*, **8**, 225-294
- FAUST G.T. and FAHEY J.J. (1962) - *The serpentine-group minerals*. U.S. Geol. Sur. Prof. Paper, **384**, 92 pp.
- MELLINI M., FUCHS Y., VITI C., LEMAIRE C. and LINARES J. (2002) - *Insights on the antigorite structure from Mössbauer and FTIR spectroscopies*. *Eur. J. Mineral*, **14**, 97-104.
- PHILIPPE J.P., ISABELLE D., KENNETH T., KOGA BRUNO R. HERVÉ CARDON and WILSON A. CRICHTON (2005) - *Kinetics of antigorite dehydration: A real-time X-ray diffraction study*. *Earth Planet. Sci. Lett.*, **2361**, 899-913
- PRIETO A.C., DUBESSY J. and CATHELINÉAU M. (1991) - *Structure-composition relationships in trioctahedral chlorite; a vibrational spectroscopy study*. *Clays Clay Min.*, **39**, 531-539
- ROY D.M. and ROY R. (1955) - *Synthesis and stability of minerals in the system MgO-Al<sub>2</sub>O<sub>3</sub>-SiO<sub>2</sub>-H<sub>2</sub>O*. *Am. Mineral.*, **40**, 147-178.
- RUSSELL J.D. and FRASER A.R. (1994) - *Infrared methods*. In: *Clay Mineralogy* (M.J. Wilson, ed.). Chapman and Hall, London, 11-67.
- SEIPOLD U. and SCHILLING F.R. (2003) - *Heat transport in serpentinites*. *Tectonophysics*, **370**, 1-4, 147-162.
- STUBICAN V. and ROY R. (1961) - *A new approach to assignment of infrared absorption band in layer structure silicates*. *Zeitschrift für Kristallographie*, **115**, 200-214.
- TAYLOR H.F.W. (1962) - *Homogeneous and inhomogeneous mechanisms in the dehydroxylation of minerals*. *Clay Mineral. Bull.*, **5**, 45-55.
- ULMER P. and TROMMSDORFF V. (1995) - *Serpentine stability to mantle depths and subduction related magmatism*: *Science*, **268**, 858-861.
- VILLIERAS F., YVON J., FRANCOIS M., CASES J.M., LHOTE F. and URIOT J.P. (1993) - *Micropore formation due to thermal decomposition of hydroxide layer of Mg-chlorites: Interactions with water*. *Appl. Clay Sci.*, **8**, 147-168.
- WARDLE R. and BRINDLEY G.W. (1972) - *The crystal structure of pyrophyllite, 1Tc and of its dehydroxylate*. *Am. Mineral.*, **57**, 732-750.
- WHITTAKER F. and ZUSSMAN J. (1956) - *The characterization of serpentine minerals by X-ray diffraction*. *Mineral Mag.*, **31**, 107-126.

